CHARACTERISTIC OF LANDSLIDE IN SEULAWAH ROAD KM 80-81, BASED ON GEOPHYSICAL DATA AND GEOTECHNICAL PARAMETERS

Zul Fadhli [1*], Etian Wirsya [1], Yurda Marvita[1], Layna Miska[1], Muhammad Syukri[2], Khalif AlFaiz[3]

[1]Geophysical Engineering, Engineering Faculty – Universitas Syiah Kuala
[2]physics Department, Faculty of Science – Universitas Syiah Kuala
[3]CV. Geotama Multi Resource
e-mail : zulfadhli@usk.ac.id

Abstrak. Penelitian ini berfokus pada pengidentifikasian bidang geser di sepanjang Jalan Seulawah (km 80-81), Muara Tiga, Kabupaten Pidie, di mana terjadi longsor besar pada tahun 2023. Dengan menggunakan metode Multichannel Analysis Surface Waves (MASW), penelitian ini mengintegrasikan data kecepatan gelombang geser (Vs) dengan nilai N-SPT dan kapasitas dukung tanah untuk menganalisis karakteristik bawah permukaan. Dengan menggabungkan pendekatan geofisika dan geoteknik, penelitian ini bertujuan untuk mengkarakterisasi bidang geser dan zona lemah yang terkait. Interpretasi menunjukkan adanya lapisan massa geser yang terdiri dari material kerikil berpasir pada kedalaman 1-3 meter dengan nilai Vs berkisar 60-150 m/s. Di bawahnya, bidang geser diinterpretasikan sebagai lapisan tanah liat kaku dengan nilai Vs berkisar 155-450 m/s pada kedalaman 6-10 meter. Kapasitas dukung tanah juga selaras dengan temuan ini dengan nilai 20-80 kN/m² pada lapisan pasir kerikil yang tidak kompak. Kapasitas dukung tanah lapisan geser, yaitu lapisan tanah liat, memiliki nilai 250-311 kN/m². Temuan ini memberikan gambaran sangat penting tentang karakteristik longsor dan menekankan ketidakstabilan dinamis lapisan geser. Selain itu, studi ini berkontribusi dalam menilai parameter kritis untuk upaya rekonstruksi masa depan dan pemeliharaan jalan, memberikan referensi penting bagi wilayah rawan longsor.
Kata Kunci: *Daya Dukung Tanah; N-SPT; Landslide; MASW; Seulawah*

Abstract. *This study identifies the sliding plane along the Seulawah Road (km 80-81), Muara Tiga, Pidie Regency, where a massive landslide occurred in 2023. Using the Multichannel Analysis Surface Waves (MASW) method, this research integrates shear wave velocity (Vs) data with N-SPT values and soil-bearing capacity to analyze subsurface characteristics. The study aims to characterize the sliding plane and associated weak zones by combining geophysical and geotechnical approaches. The interpretation reveals the existence of a sliding mass layer consisting of sandy gravel material at a depth of 1-3 meters with a Vs value in the range of 60-150 m/s. Underneath that, the sliding plane is found, which is interpreted as a stiff clay layer with the Vs value in the range of 155-450 m/s at a depth of 6-10 meters. The soil bearing capacity also aligned with these findings with the 20-80 kN/m2 value in the very loose sandy gravel layer. The soil-bearing capacity of the sliding plane, the clay layer, is 250-311 kN/m2. Those findings provide valuable insights into landslide characteristics and highlight the dynamic instability of the sliding plane. Moreover, this study contributes to assessing critical parameters for future reconstruction and road maintenance, offering an essential reference for landslide-prone regions.*
Keywords: *Soil bearing; N-SPT; Landslide; MASW; Seulawah.*

INTRODUCTION

Each year, Landslides lead to significant social disturbances and financial losses, with immediate and long-term consequences (Turner, 2018). Landslides are motions down a slope of rock mass, soil, or debris driven by gravity that cause inevitable losses such as economic or casualties (Tehrani *et al.*, 2022). Indonesia is in a tropical climate area prone to major landslide incidents due to the high rainfall and variable geological situation (Darman, 2018; Syukri *et al*., 2020a; Ismail *et al.*, 2014). According to Indonesian National Disaster Management Agency (BNPB) statistical data, 9,820 landslides occurred until recently. In 2024, there were already about 183 reported from January to April.

Landslides generally occur when geological conditions include rock formations capable of functioning as either the sliding plane or the layer comprising the sliding mass (Andika *et al.*, 2024). The sliding plane layer is the interface between the stable ground and the moving landslide mass facilitating the shear displacement. Meanwhile, the landslide mass layer comprises distinct materials, including original rocks or soil and any

DOI : http://dx.doi.org/10.12962/j25023659.v11i4.5122

Artikel Masuk : 14-06-2025 Artikel Diulas : 19-06-2025 Artikel Diterima : 11-08-2025

entrained debris that slides down the slope during a landslide (Tao *et al.*, 2020; Maulia *et al.*, 2022). Sliding planes are often associated with high water content and weathering in specific geological layers (Pratiwi *et al.*, 2019; Purnamasari *et al.*, 2024). The Aceh Department of Energy, Resources, and Minerals (ESDM Aceh) has proposed the hypothesis that the landslide occurred in the research area along the Seulawah Main Road at km 80-81. The landslide is believed to have been caused by the swelling in the highly weathered layer (esdm.acehprov.go.id, 2023).

Several scientific methods have been used to analyze landslides including Machine learning (He *et al.*, 2019), material point method (Soga *et al.*, 2018), CPT (cone penetration test), and SPT (standard penetration test) (Rusydy *et al.*, 2017). Geophysical methods are often involved such as Seismic Refraction (Syukri *et al*.,2020b; Fadhli *et al*., 2022), UAV (Hussain *et al.*, 2022), GPR and ERT (Syukri, *et al.*,2022), also HVSR and ANI, despite the last two are not much effective in practice (Hussain *et al.*, 2019).

Over the past 20 years, the MASW method, a non-destructive seismic technique has been widely used for soil characterization. It was primarily developed for shallow geophysical investigations (Al-Heety, 2021). The MASW method delivers reliable data for quality control and monitoring by accurately assessing material dynamic stiffness, which is critical in the construction and maintenance of road infrastructure, without providing damage to surrounding (Park *et al.*, 2018). Aside from imaging the subsurface using the shear wave velocity variation, the MASW (Multichannel Analysis Surface Wave) method is use in this case to analyze geotechnical parameters, specifically soil bearing capacity values which correlated directly to soil compaction that can trigger roadway landslide (Mitu *et al.*, 2020). This method facilitates the determination of subsurface shear wave velocity (Vs) effectively, which exhibits variability based on the underlying rock types (Ivanov *et al.*, 2015).

In purpose of connecting the soil bearing capacity value with the information of Vs found, several empirical expressions that had been proposed by a number of researchers are used (Tezcan and Ozdemir, 2012; Supriyatno, 2022). To validate the results, N-SPT data were utilized as additional combination, serving as a key reference for determining the soil type. The object of this study is to derive a new relationship between soil-bearing capacity and shear wave velocity (Vs). Data acquisition was explicitly focused on locations with a high potential for landslides. These locations are also situated in the volcanic region of Mount Seulawah, which has complex geological conditions. The geological conditions at these locations include pyroclastic layers, volcanic ash, and water-saturated clay layers. Such soil characteristics significantly influence both the Vs value and soil-bearing capacity. Therefore, the empirical relationship obtained from this study is expected to describe the mechanical response of soil to external influences. It is hoped that these results will serve as a reference for slope stability analysis in geotechnical design in areas with geological complexity.

GEOLOGICAL SETTING

In general, this research is located on high topography and steep slopes. Landslides are occurring in this location and are predicted to continue due to several external factors (figure 1). Looking at the overall scope of the Area, the geological framework of Pidie is primarily characterized by a sequence of pre-Tertiary rocks, Quaternary sediments, Tertiary formations, volcanic rocks, and intrusive igneous bodies. Based on the geological map sheet displayed in Figure 2 reveals that the research area is located in the Lam Teuba formation (QTvt), which consists of andesitic to dacitic volcanic rocks, pumiceous breccias, tuffs, agglomerates, and ash-flows from the Pleistocene era, as well as mud-flows on top of these volcanic rocks which deposited during the Holocene epoch (Zaini *et al.*, 2021).

DOI : http://dx.doi.org/10.12962/j25023659.v11i4.5122

Artikel Masuk : 14-06-2025 Artikel Diulas : 19-06-2025 Artikel Diterima : 11-08-2025

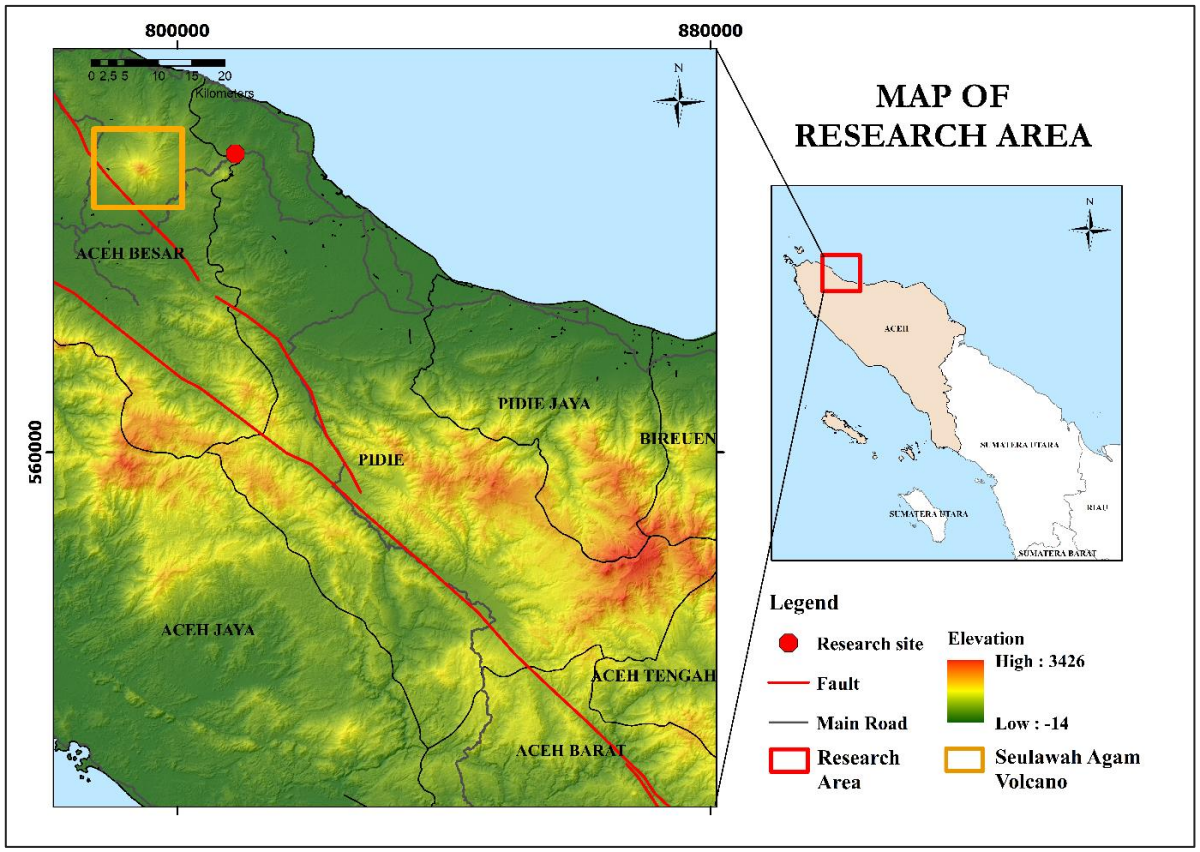

Figure 1. Map of Research Area

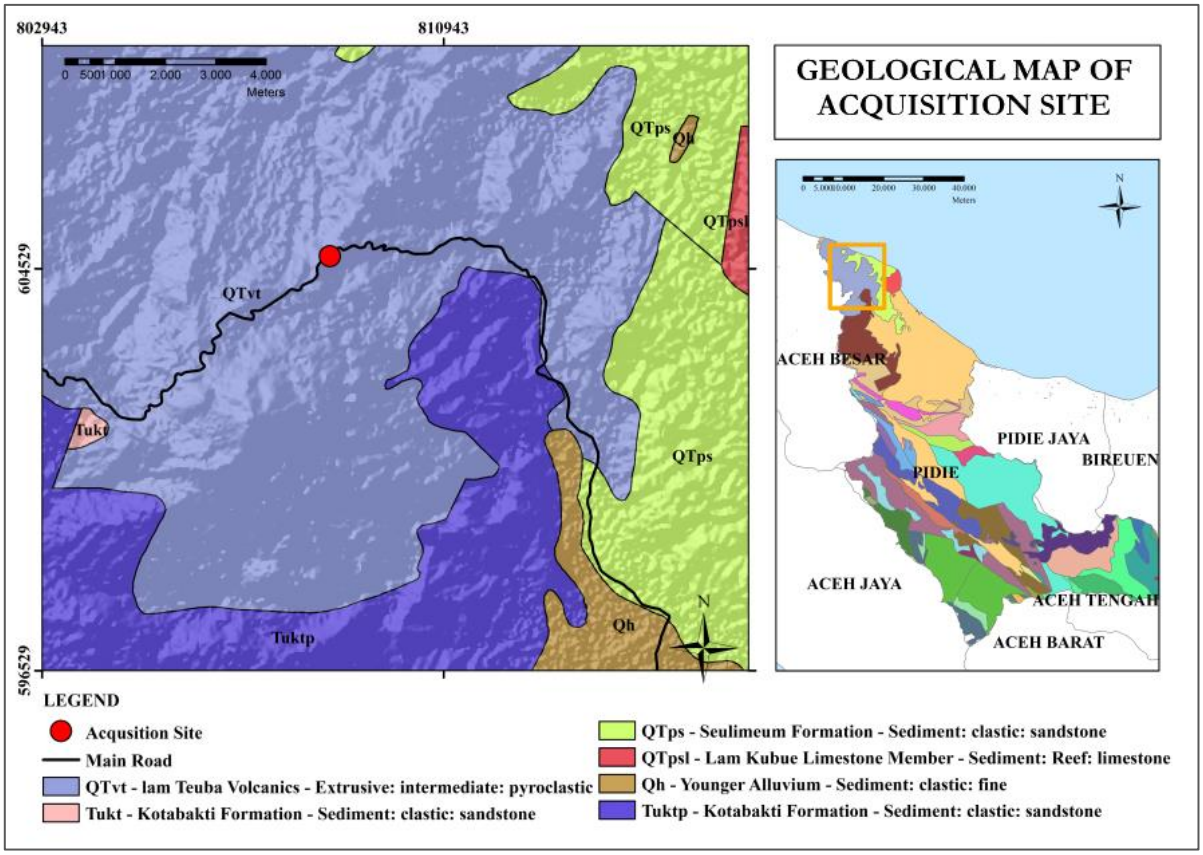

Figure 2. Geological Map of acquisition site

DOI : http://dx.doi.org/10.12962/j25023659.v11i4.5122

Artikel Masuk : 14-06-2025 Artikel Diulas : 19-06-2025 Artikel Diterima : 11-08-2025

METHODOLOGY

The research was conducted in the landslide-prone area of the Seulawah road, Muara Tiga, Pidie Regency, following a series of systematic steps. The process began with a literature review, such as geological study, focused on the region to identify the factors contributing to the occurrence of landslides.

The subsequent phase involved conducting field data acquisition using the MASW method, which was selected for the study. The field measurements were carried out using a PASI 16S-24P Seismograph connected to 24 4Hz geophones, with a sledgehammer serving as the seismic energy source. Data was collected along two measurement lines, each 48 meters long, as shown in Figure 3. The distance between the two lines is 50 meters with almost similar topography. These two lines were arranged parallel to each other to enable comparison between them. These lines were also arranged perpendicular to the landslide location to obtain a detailed cross-section of the landslide's direction and plane. Geophones with a frequency of 4 Hz were installed on these lines at intervals of 2 meters, producing a total of 14 measurement points for data collection, as shown in Figure 4. At each shootpoint, the source was activated 9 times to obtain a clear visualization of the shear wave. The geophone trigger was placed at the edge of the source plate. Its position is kept as close as possible to capture the vibrations immediately. The source is applied when noise (vehicle movement and wind) is considered absent

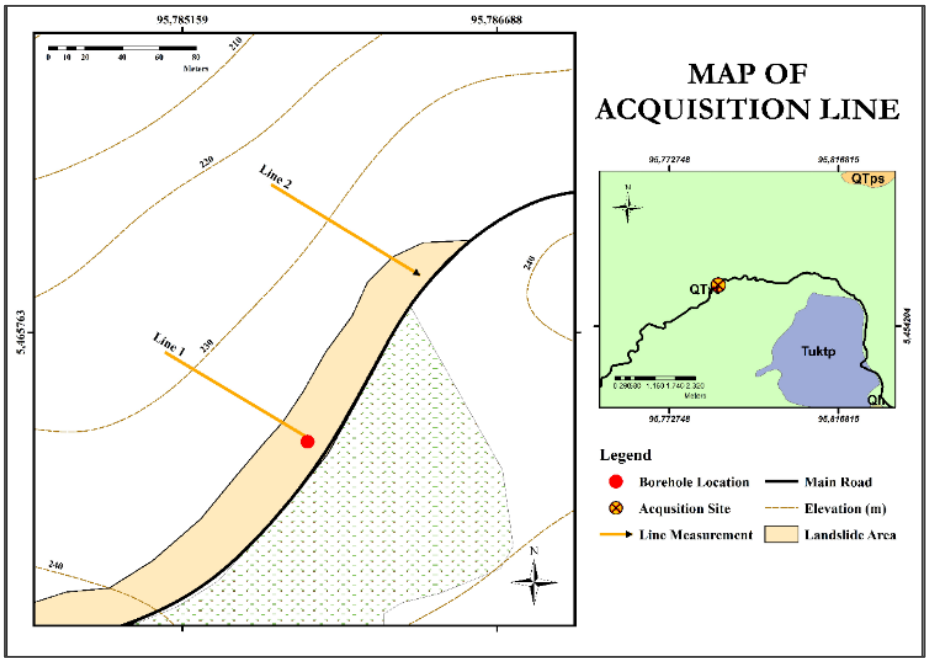

Figure 3. Map of Acquisition Lines

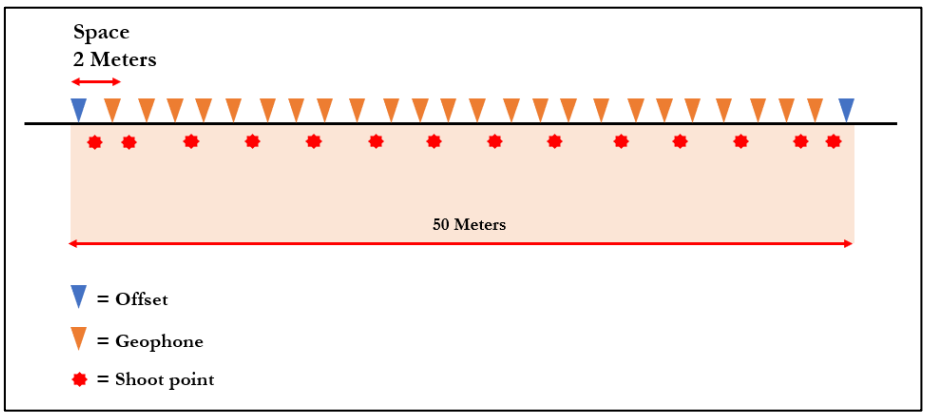

Figure 4. Measured acquisition line geometry

DOI : http://dx.doi.org/10.12962/j25023659.v11i4.5122

Artikel Masuk : 14-06-2025 Artikel Diulas : 19-06-2025 Artikel Diterima : 11-08-2025

Data Processing and modelling

The data processing was conducted using SeisImager software, following a series of key steps to generate both 1D and 2D subsurface models. These steps included: (1) identifying the S-wave for each recorded shot point, (2) generating dispersion curves for shear wave velocity (Vs), (3) performing an inversion of each dispersion curve to derive Vs variations with depth, and (4) constructing 1D and 2D subsurface models based on the processed data (5) analyzing and interpret the data (Al-Heety, 2021).

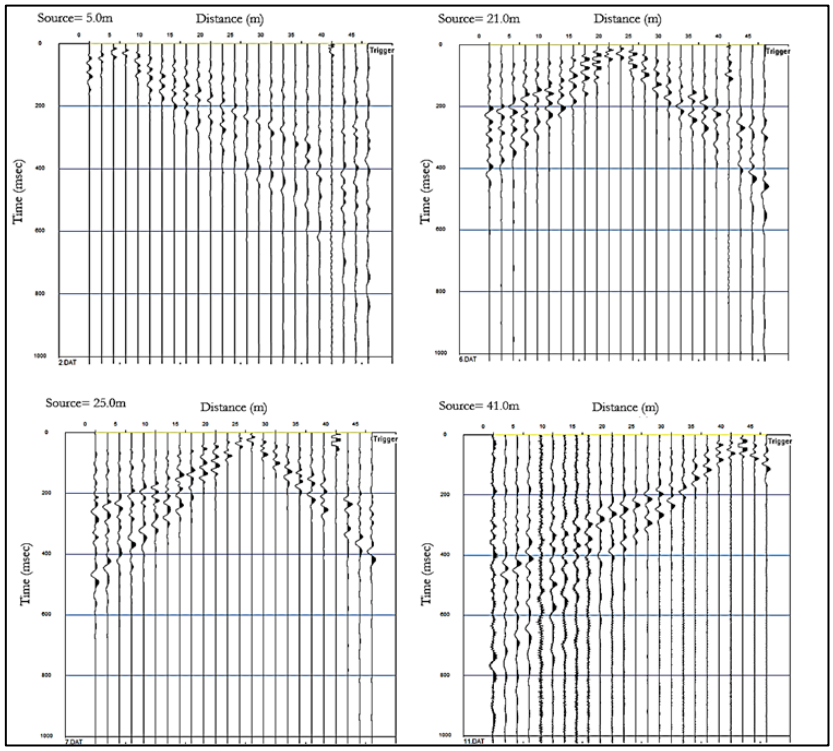

Figure 5. Selected dispersion waveform samples of line 1.

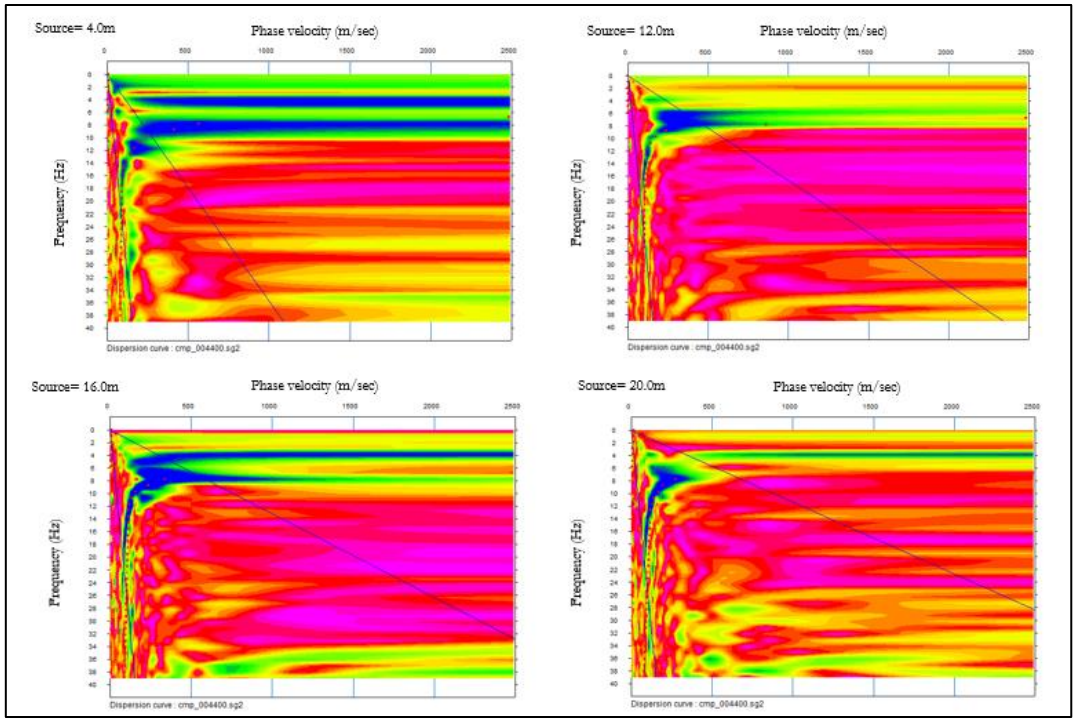

Figure 6. Selected dispersion curves sample of shoot points at 4, 12, 16, and 20 meters of line 1

DOI : http://dx.doi.org/10.12962/j25023659.v11i4.5122

Artikel Masuk : 14-06-2025 Artikel Diulas : 19-06-2025 Artikel Diterima : 11-08-2025

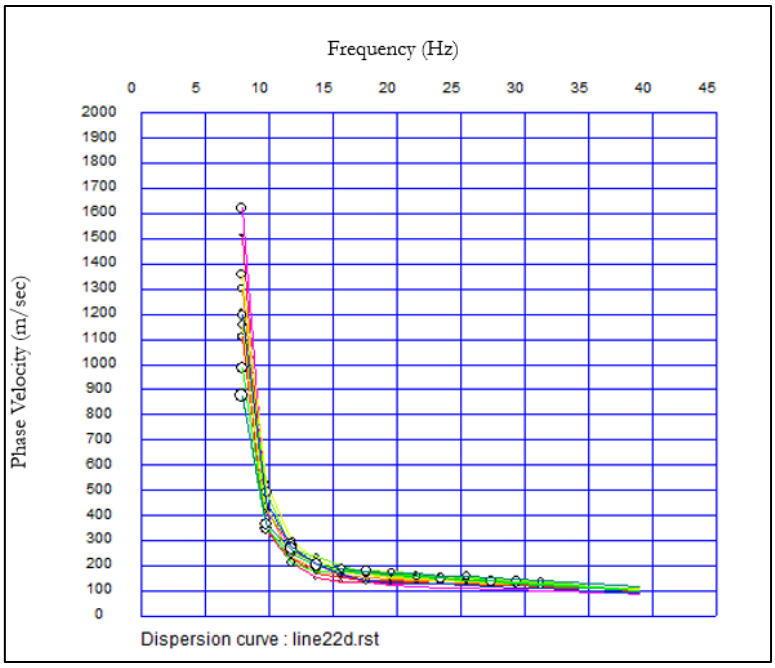

Figure 7. dispersion curves of line 1 combined after picking process

The selected waves of line 1 can be seen in figure 5 and 6. Each serves as comparison between the observed waveforms obtained from in-situ acquisition (figure 5) and the change of wave signal based on the dispersive behavior of the shear wave velocity (figure 6). The four samples of waveform and dispersion signal in each Figure 5 and 6 were chosen as it gives better quality signals that are easier to observe. After the dispersion curves was picked, the result produced clean and well-defined curves, as shown in figure 7.

Soil Bearing Capacity Identification Using Vs

The result of processing is consisting of 1D and 2D models of the S-wave velocity to depth. The shear strength of soil layers is directly related to their bearing capacity. A reduction in shear strength can significantly compromise overall stability and soil bearing capacity, potentially accelerating the occurrence of landslides (Yerro *et al*, 2016; Chwała and Puła, 2020). By using shear wave velocity obtained, we can imaging the subsurface to find the potential sliding plane layer and determine its value of soil bearing capacity (Tezcan *et al*, 2009). Several empirical expressions were employed to determine the soil bearing capacity value in this study. The material utilized was initially established by Tezcan *et al*. in 2009 with an updated version released in 2012. Soil bearing capacity (*qa*) is calculated by dividing the value of ultimate bearing capacity at failure (*qf*), with the safety factor of 'n' as written below.

$$q_a = \frac{q_f}{n} \tag{1}$$

With,

$$q_f = \gamma H \tag{2}$$

thus,

$$q_a = \frac{\gamma H}{n} \tag{3}$$

To correlate the expression with the S-wave velocity obtained by the in-situ MASW acquisition, the following equation was stated as,

DOI : http://dx.doi.org/10.12962/j25023659.v11i4.5122

Artikel Masuk : 14-06-2025 Artikel Diulas : 19-06-2025 Artikel Diterima : 11-08-2025

$$H = V_s\, t \tag{4}$$

therefore,

$$q_a = \frac{\gamma\, V_s\, t}{n} \tag{5}$$

The factor of safety (n) and time (t) has been determined according to several thorough examination by Tezcan, *et al* (2006), which stated the use of *n* in the range of 1.4 - 4.0 based on the Vs value, and the use of t constant of 0.10 s. With the value calculated, the relation between Vs and soil *qa* can be observed refer to Table 1. The table below contained the variety ranges of allowable bearing capacity for each soil classes, cohesive and granular (Tezcan *et al*, 2009). The allowable values listed in the table are for static load conditions only. This table does not consider groundwater conditions, the conductivity of a formation, or dynamic loads (external factors) such as earthquakes or repeated loads.

Table 1. Allowable Soil Bearing Capacity Value for soil categories (Tezcan *et al*, 2009)

Soil Type	**Vs-Range**	**q_a**
Cohesive	**m/s**	**kPa**
Very soft clay & silts	0-100	0-50
Soft clay & silts	0-200	0-75
Medium stiff clays	200-350	75-150
Stiff clays	200-600	100-250
Very stiff clays/boulders	450-800	200-350
Hard clays, boulders	600-900	250-400
Very hard clays	800-1200	350-500
Granular Soil		
Very Loose Sand	0-100	0-50
Loose sand and gravel	100-350	50-100
Medium dense sand, gravel	250-700	100-300
Dense sand and gravel	600-1100	250-450
Very dense sand and gravel	800-1500	350-600

The result of the calculation settled the value of the allowable bearing capacity of each lithology layer. The outcome of this research will include a Shear wave velocity model of the subsurface in the landslide-prone area, along with the allowable bearing capacity values for each Vs value that represent each layer. This data is used to help characterized the landslide which can serve as a critical geotechnical reference for ensuring the stability of any foundation during construction (Mirsayapov *et al,* 2021).

RESULTS AND DISCUSSION

Table 2 provides the value of N-SPT of each soil layer up to the depth of 20 meters consisting of 11 layers. This data was collected subsequent to the landslide and about two months prior to the MASW acquisition. The Borehole for the N-SPT data is located at the far end of Line 1 as shown in Figure 3. Since Line 2 does not have the test occurred around it, the interpretation is correlated to Line 1, considering the relatively acceptable distance of approximately 48 meters between the two lines. This condition allows for reasonable correlation.

Examining the table, we can recognize a pretty much noticeable value dip at the approximate depth of 5 meters, where the number decrease from 35 to 21. This transition suggests a change in soil type or composition from what likely assumed to be sandy gravel with medium density, to clay which is stiff in consistency. Such decrease may indicate the reduction in the static stiffness of the soil layer. At the depth of 12-20 meters, the layer that consists of marl is located. This change marked by significant increase of the N-SPT value from 31 to 59-60. This layer considered very dense with low moisture rate, a contrast to the previous.

DOI : http://dx.doi.org/10.12962/j25023659.v11i4.5122

Artikel Masuk : 14-06-2025 Artikel Diulas : 19-06-2025 Artikel Diterima : 11-08-2025

Table 2. the soil/rocks layers characteristics based on the value on N- SPT (standard penetration test)

Depth (m)	Soil/ Rocks Characteristics	N-SPT
0 - 0,60	Clay (reddish-brown color)	0
0,60 – 2,00	Sandy Gravel (dark grey, non-plastic, medium density, moderate moisture content).	33
4,00		35
6,00	Clay (yellowish-brown, medium plasticity, stiff consistency, moderate moisture content).	21
8,00		24
10,00		31
12,00	Marl (yellowish-grey, non-plastic, very dense, low moisture content).	59
14,00		60
16,00		60
18,00		60
20,00		60

The N-SPT data can be aligned with the Vs behavior observed from the models obtained after completing the MASW data processing sequences. Figure 8, 9, and 10 present the 1D and 2D of the shear wave velocity model derived from the in-situ acquisition. The 1D models illustrate the Vs values for each layer down to the depth 35 meters. The two selected 1D models are from the distance of 20 meters, to provide data at median distance. We can clearly see the dip of Vs value on 1D model in the depth of 1-5 meters which presumably corresponding to the sandy gravel layer, reaching the range of 60-120 m/s in Line 1 (Figure 8a), and 90-120 m/s in Line 2 (Figure 8b), indicating a relatively soft soil layer. Beneath this, a layer with slightly higher Vs value range of 150-450 m/s is found. Which from SPT data, is classified as clay layer. The samples are selected based on their accessibility on observation, as they represented an intermediate distance.

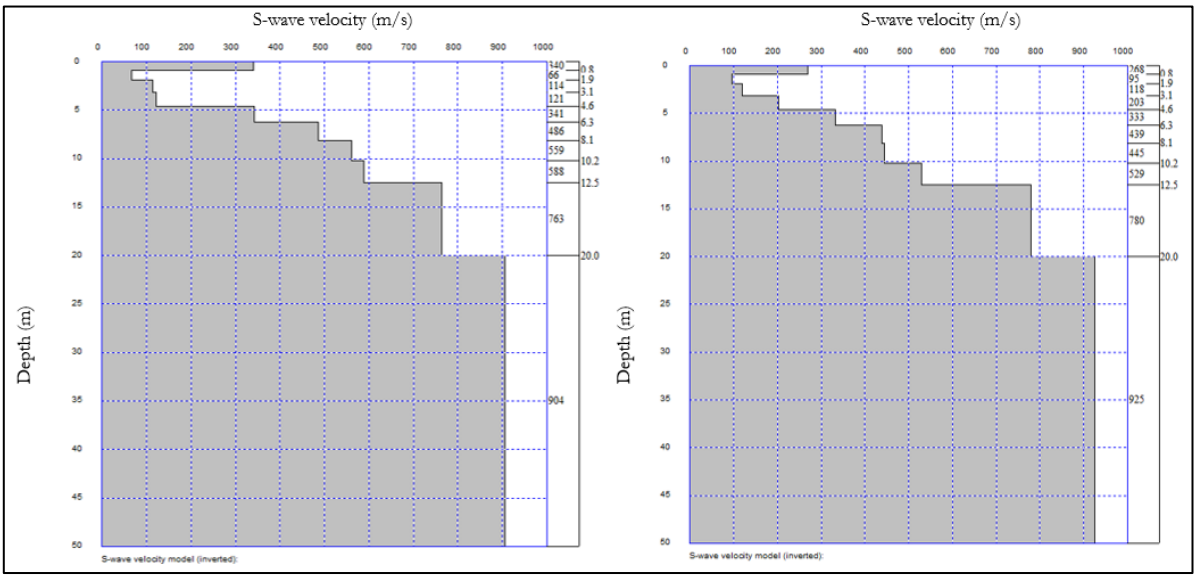

Figure 8. Samples of 1D model of line 1 (a), and line 2 (b), from the distance of 20 meters (about center).

The 2D models, as shown in Figure 9 and 10, corroborate the Vs ranges observed in 1D models, with similar velocity trends and layer characteristic. In these models, the observed decrease and increase are effectively highlighted through the variation in color across the layers. In the line 1 model (Figure 9), the layer transitions from a red to a lighter shade (pink) at a depth approximately 1-5 meters, particularly around the distance of 24 meters mark (center of the section). The Line 2 model (Figure 10) exhibits a comparable

DOI : http://dx.doi.org/10.12962/j25023659.v11i4.5122

Artikel Masuk : 14-06-2025 Artikel Diulas : 19-06-2025 Artikel Diterima : 11-08-2025

behavior, though the transition is less pronounced. These models also reveal a slightly deeper layer, at a depth of 6-10 meters, where the color morphs from red to a greenish hue.

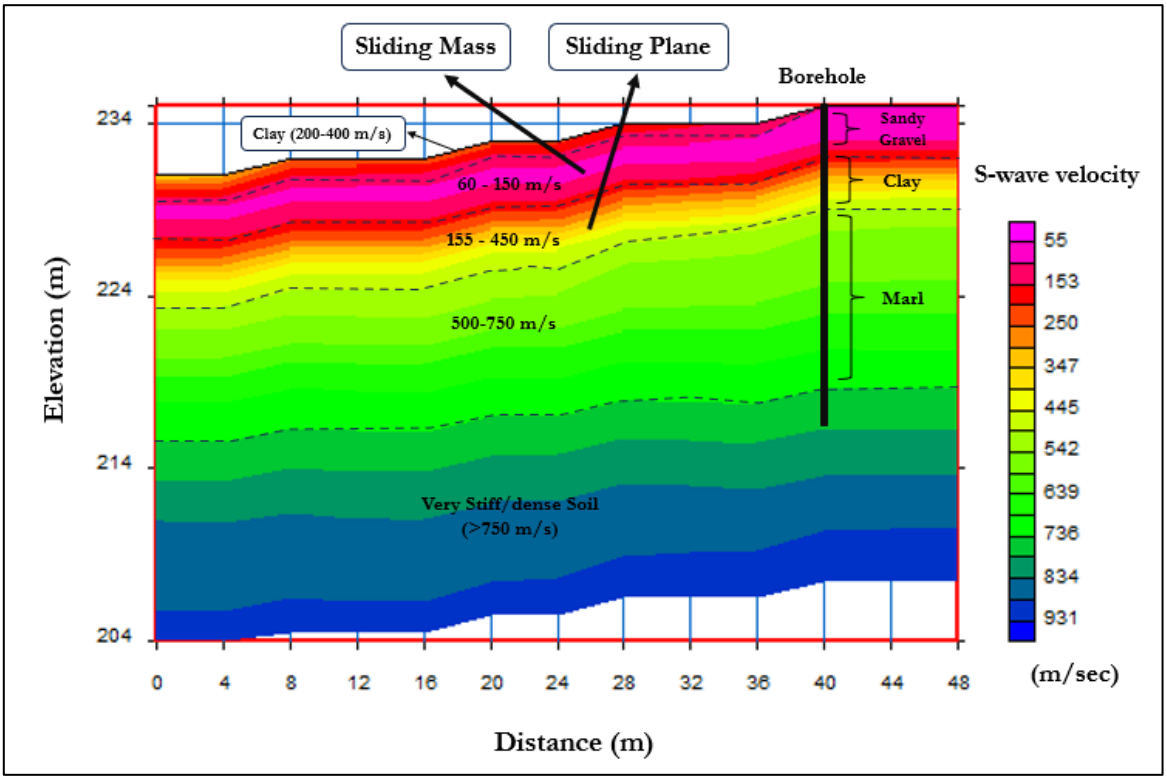

Figure 9. The 2D Subsurface Shear Wave Velocity Model of Line.

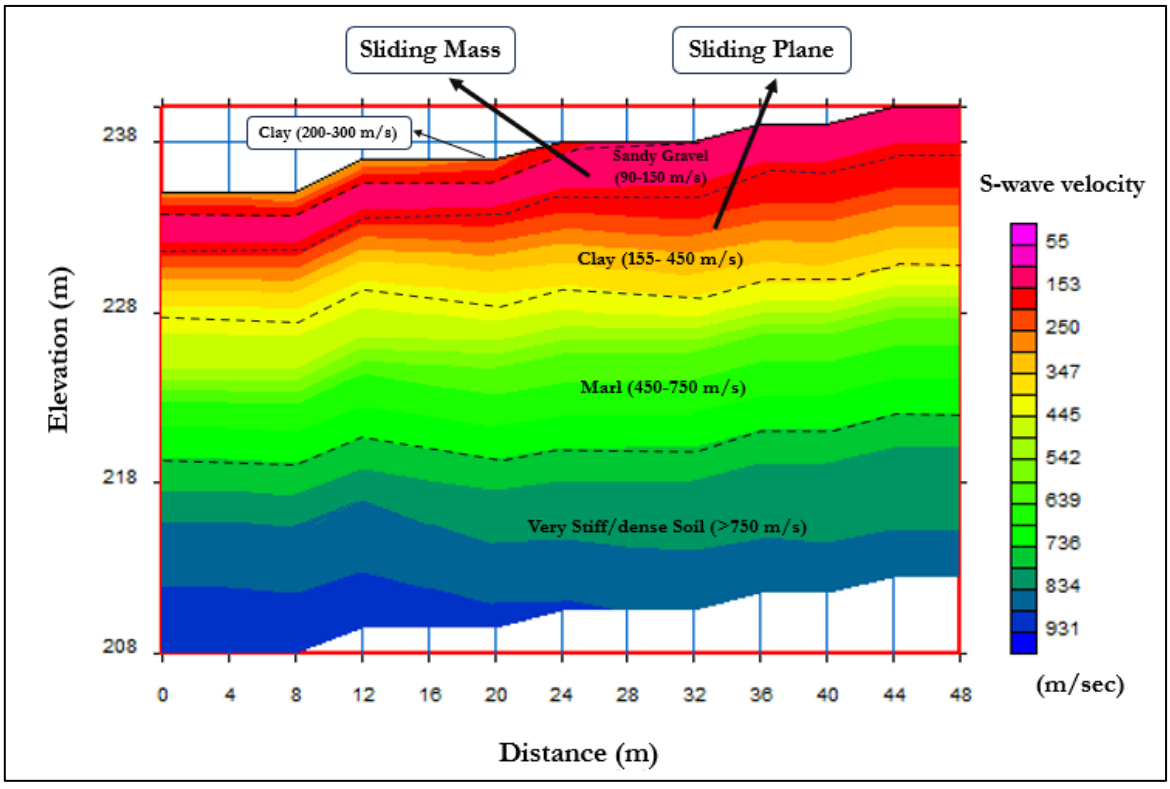

Figure 10. The 2D Subsurface Shear Wave Velocity Model of Line 2.

DOI : http://dx.doi.org/10.12962/j25023659.v11i4.5122

Artikel Masuk : 14-06-2025 Artikel Diulas : 19-06-2025 Artikel Diterima : 11-08-2025

In this case, by integrating the SPT field test result (Table 2) with the Vs-to-soil-type correlations (Table 1), it can be deduced that the overlying loose sandy gravel layer constitutes the sliding mass, while the stiffer clay layer beneath it serves as the sliding plane. Having established the role of the significant layers, it is essential to further evaluate the mechanical properties of these layers, particularly their soil bearing capacity. By conducting the equation (1) to (5), the soil bearing capacity corresponding to these Vs layers are achieved. The detailed soil bearing capacity value to depth data is provided in Table 3, offering the value of each Vs Layers to depth, soil bearing capacity, and the N-SPT value that relate both Lines.

Table 3. The correlation among Soil Bearing Capacity, Vs Value, and N-SPT value

	Depth (m)	Vs (m/s)	qa (kN/m2)	N-SPT		Depth (m)	Vs (m/s)	qa (kN/m2)
LINE 1	0.5	340	157	0	LINE 2	0.5	268	117
	1	66	20			1	95	32
	2	114	40	33		2	118	42
	3	121	43			3	203	82
	5	341	158	35		5	333	153
	6	486	245	21		6	439	216
	8	559	292	24		8	445	220
	10	588	311	31		10	529	273
	12	763	432	59		12	780	446
	20	904	550	60		20	925	568

From the table given, we can analyze the correlation between the data to the soil bearing capacity. In the depth of 6-10 meters, which where the sliding plane clay layer is presumably located, the bearing capacity increased to a higher value of 250-320 kN/m^2 in line 1, and the range of 220-300 kN/m^2 in Line 2**.** In the sliding mass layer of sandy gravel at the depth of 1-5 meters, the soil bearing capacity value lessen to the range of 20-158 kN/m^2 in Line 1**,** and 32-153 kN/m^2 in Line 2. Thus, sealed the distinct correlation between the N-SPT data, the Vs value, and the Soil Bearing Capacity.

Though, there is an interesting discrepancy among these data which require a thorough analysis. Despite the Vs value aligned perfectly along the Soil bearing capacity, the N-SPT data show a contrast behavior in indicating that there is a weaker resistance in clay layer depth by moderate values of 21-31 which has been named the assumed sliding plane, rather than the sandy gravel layer which shown the value of 33-35 as the sliding mass (Syukri *et al*, 2021). This discrepancy can be attributed to differences in data interpretation methods. SPT (Standard Penetration Test) reflects soil static resistance to penetration under specific impact force throughout a dynamic test (Zhang *et al.*, 2021). Different from Vs which focuses on the soil elastic properties under small-strain, and the ability of soil to resist shearing motion under dynamic conditions (Tunusluoglu, 2023).

Thus, despite the sliding mass layer of sandy gravel is higher in N-SPT value, it is not necessarily stated that the soil will be high on shear wave velocity too. Sandy gravel layers typically exhibit high porosity and low cohesion due to their larger grain sizes compared to finer soils like clay or silt (van Lopik *et al.*, 2020). That also defining the difficulty in the penetration process, since the split barrel sample could hit larger pebbles. Plus, the location of the layer that is close to the surface may increase the risk of it being saturated more by water and weather. That explained the low Vs value and high N-SPT.

The Clay layer that exhibits a lower SPT value, are consisting of very stiff Clay which easily pierced in penetration test because of the cohesive properties that structured the layer. However, the uniformity also strengthens the bind inter-grains. Despite prone to higher load or specific impact, the layer show behavior of high strength toward shear stress (Yu *et al*, 2024). Hence the high Vs value and low N-SPT. Through this analysis, we can safely assume that the sliding plane is located in the clay layer, with the sandy gravel layer

DOI : http://dx.doi.org/10.12962/j25023659.v11i4.5122

Artikel Masuk : 14-06-2025 Artikel Diulas : 19-06-2025 Artikel Diterima : 11-08-2025

on top of it as the sliding mass should another landslide occurred. This mechanism is consistent with classical landslide models where a weak, cohesive layer underlies a less cohesive but unstable mass.

CONCLUSION

The analysis of N-SPT data, shear wave velocity (Vs) models, and soil bearing capacity has provided valuable insights into the characteristics of the sliding plane and subsurface conditions. The study integrates these three parameters to analyze the characteristics of the Landslide, Seulawah Road km 80-81, Muara Tiga, Pidie Region. The N-SPT data and the shear wave velocity (Vs) models provide the insights into the mechanical behavior of soil layers up to 20 meters deep. A noticeable decrease in N-SPT values at approximately 5 meters suggests a transition from sandy gravel (N-SPT: 33-35) to clay (N-SPT: 21-31), indicative of reduced stiffness. The 1D and 2D Vs models (Figure 8-10) corroborate the transitions, showing low Vs values (60-120 m/s) for the sandy gravel layer and higher Vs values (150-450 m/s) for the underlying clay. Using the N-SPT and Vs data correlations, it is inferred that the sandy gravel layer acts as the sliding mass, while the stiff clay layer acts the sliding plane.

Soil bearing capacity, calculated from Vs data, further supports this interpretation (Table 3). The clay layer, identified as the sliding plane, exhibits higher bearing capacity values (250-320 kN/m^2 in line 1 and 220-300 kN/m^2 in line 2) despite lower N-SPT values. This discrepancy arises due to the differing measurement principles of N-SPT and Shear wave Velocity: N-SPT measures static resistance to penetration, while Vs reflects dynamic elastic properties. The soil type also contributes to the discrepancy. Sandy gravel with higher N-SPT values is less stable due to low cohesion, high porosity and saturation potential, while the cohesive clay layer, though easier to penetrate, exhibits a greater shear strength, aligning the classical landslide models where unstable masses overlay weaker, cohesive layer. Thus, identifying the clay as the sliding plane and the sandy gravel layer as the sliding mass in potential landslide.

Acknowledgment

First and foremost, the authors would like to express gratitude to the Geophysical Near Surface Laboratory Staff for facilitating the research. Special appreciation is extended to the Geophysical department students and all members of the acquisition team for their invaluable support in the field.

REFERENCES

Al-Heety, A.J.R. (2021). Application of MASW and ERT methods for geotechnical site characterization: A case study for roads construction and infrastructure assessment in Abu Dhabi, UAE, *Journal of Applied Geophysics*, 193(July), p. 104408. https://doi.org/10.1016/j.jappgeo.2021.104408.

Anbazhagan, P., Uday, A., Moustafa, S, S, R., Al-Arifi, N, S, N., (2016). Correlation of densities with shear wave velocities and SPT N values, *Journal of Geophysics and Engineering*, Vol.13, No.3, pp. 320–341. https://doi.org/10.1088/1742-2132/13/3/320.

Andika, M.A., Minardi, S., and Marzuki., (2024). Detection and Identification of Sliding Planes using Geoelectric Methods at Bengkaung Toursm Area, Lombok Island, Indonesian Physical Review, *Indonesian Physical Review*, 7(3), pp. 350–360. https://doi.org/10.29303/ipr.v7i3.302

Chwała, M., and Puła, W., (2020). Evaluation of shallow foundation bearing capacity in the case of a two-layered soil and spatial variability in soil strength parameters, *PLoS ONE*, Vol.15, No.4, pp. 1–23. https://doi.org/10.1371/journal.pone.0231992.

Darman, R., (2018). Pembangunan Dashboard Lokasi Rawan Tanah Longsor di Indonesia Menggunakan Tableau, *Jurnal Teknik Informatika dan Sistem Informasi*, Vol.4, No.2, pp. 254–267. http://114.7.153.31/index.php/jutisi/article/view/1493.

ESDM (2023). *Begini Analisis Tim Geologi Dinas ESDM Aceh Terkait Jalan Ambles di KM 80*. Accessed 3 August 2024 from: https://esdm.acehprov.go.id/berita/kategori/esdm-aceh/begini-analisis-tim-geologi-dinas-esdm-aceh-terkait-jalan-ambles-di-km-80.

Artikel Masuk : 14-06-2025 Artikel Diulas : 19-06-2025 Artikel Diterima : 11-08-2025

Fadhli, Z., Anda, S, T., Syukri, M., Karmel, M, E, R., Tutifla, A, S., Hasibuan, P., Safitri, R., (2022). Ground Surface Quality Assessment Using P-Wave Velocity From 2-D Seismic Refraction Method. Aceh International Journal of Science and Technology, 11(3), 258-265. https://doi.org/10.13170/aijst.11.3.28818

He, Q., Shahabi, H., Shirzadi, A., Li, S., Chen, W., Wang, N., Chai, H., Bian, H., Ma, J., Chen, Y., Wang, X., Chapi, K., Ahmad, B, B., (2019). Landslide spatial modelling using novel bivariate statistical based Naïve Bayes, RBF Classifier, and RBF Network machine learning algorithms, *Science of the Total Environment*, Vol.663, pp. 1–15. https://doi.org/10.1016/j.scitotenv.2019.01.329.

Hussain, Y. Hussain, Y., Cardenas-Soto, C., Martino, S., Moreira, C., Borges, W., Hamza, O., Prado, R., Uagoda, R., Rodríguez-Rebolledo, J., Silva, R, C., Martinez-Carvajal, H., (2019). Multiple geophysical techniques for investigation and monitoring of Sobradinho Landslide, Brazil, *Sustainability (Switzerland)*, Vol.11, No.23. https://doi.org/10.3390/su11236672.

Hussain, Y., Schlögel, R., Innocenti, A., Hamza, O., Iannucci, R., Martino, S., Havenith, H., (2022). Review on the Geophysical and UAV-Based Methods Applied to Landslides, *Remote Sensing*, Vol.14, No.18, pp. 1–33. https://doi.org/10.3390/rs14184564.

Ismail, N, A., Saad, R., Saidin, M., Nordiana, M, M., Fadhli, Z., Kamarudin, N, A., (2014). ntegrating 2-D Electrical Resistivity and Moisture Content for Soil Characterization Inside Bukit Bunuh Impact Crater. *Electronic Journal of Geotechnical Engineering*, *19*, Z3.

Ivanov, J., Miller,R, D., Morton, S, L., Peterie, S., (2015). Dispersion-curve imaging considerations when using multichannel analysis of surface wave (MASW) method, *28th Symposium on the Application of Geophysics to Engineering and Environmental Problems 2015, SAGEEP 2015*, Vol.2010, pp. 489–499. https://doi.org/10.4133/sageep.28-079.

Van Lopik, J, H., Zazai, L., Hartog, N., Schotting, R, J., (2020). Nonlinear Flow Behavior in Packed Beds of Natural and Variably Graded Granular Materials, *Transport in Porous Media*, Vol.131, No.3, pp. 957–983. https://doi.org/10.1007/s11242-019-01373-0.

Maulia, I., Wibowo, R, C., Haerudin, N., Sarkowi, M., (2022). Slip Surface Identification for Landslide Hazard Mitigation with Electrical Resistivity Tomography" *Indonesian Physical Review*, Vol.6, No.1, pp. 1–10. https://doi.org/10.29303/ipr.v6i1.181.

Mirsayapov, I., Shakirov, I. and Nurieva, D. (2021). Numerical studies of soil base deformations from reconstructed multi-storey building to nearby buildings, *E3S Web of Conferences*, Vol.274. https://doi.org/10.1051/e3sconf/202127403020.

Mitu, S.M., (2020). Determination of Soil Bearing Capacity from Spectral Analysis of Surface Wave Test, Standard Penetration Test and Mackintosh Probe Test, *International Journal of Innovative Technology and Exploring Engineering*, Vol.9, No.7, pp. 340–346. https://doi.org/10.35940/ijitee.g5006.059720.

Mohammed Shafiqu, Q.S., Güler, E. and Edinçliler, A., (2018). Mechanical Parameters and Bearing Capacity of Soils Predicted from Geophysical Data of Shear Wave Velocity, *International Journal of Applied Engineering Research*, Vol.13, No.2, pp. 1075–1094.: http://www.ripublication.com.

Park, C., Richter, J., Rodrigues, R., Cirone, A., (2018.) MASW applications for road construction and maintenance, *Leading Edge*, Vol.37, No.10, pp. 724–730. https://doi.org/10.1190/tle37100724.1.

Pratiwi, E.S., Sartohadi, J. and Wahyudi., (2019). Geoelectrical Prediction for Sliding Plane Layers of Rotational Landslide at the Volcanic Transitional Landscapes in Indonesia, *IOP Conference Series: Earth and Environmental Science*, Vol.286, No.1. https://doi.org/10.1088/1755-1315/286/1/012028.

Purnamasari, A.N.C., Sartohadi, J., and Hartantyo, E. (2024). Pseudo Sliding Plane in Super-Thick Soil Materials Deposit at Ngasinan Deep Landslide Area, *Revista Brasileira de Geomorfologia*, Vol.25, No.2. https://doi.org/10.20502/rbgeomorfologia.v25i2.2540.

Rusydy, I., Al-Huda, N., Jamaluddin, K Sundari, D., Nugraha, G, S., (2017). Analisis Kestabilan Lereng Batu Di Jalan Raya Lhoknga Km 17,8 Kabupaten Aceh Besar, *RISET Geologi dan Pertambangan*, Vol.27, No.2, pp. 145–155. https://doi.org/10.14203/risetgeotam2017.v27.452.

DOI : http://dx.doi.org/10.12962/j25023659.v11i4.5122

Artikel Masuk : 14-06-2025 Artikel Diulas : 19-06-2025 Artikel Diterima : 11-08-2025

Soga, K., Alonso, E., Yerro, A., Kumar, K., Bandara, S., Kwan, J, S, H., Koo, R, C, H., Law, R, P, H., Yiu, J., Sze, E, H, Y., Ho, K, K, S., (2018). Trends in large-deformation analysis of landslide mass movements with particular emphasis on the material point method, *Geotechnique*, Vol.68, No.5, pp. 457–458. Available at: https://doi.org/10.1680/jgeot.16.D.004.

Syukri, M., Taib, A, M., Fadhli, Z., Safitri, R., (2020a). Geophysical Investigation of Road Failure the Case of The Main Street of Alue Naga, Banda Aceh, Indonesia, In *IOP Conference Series: Materials Science and Engineering* (Vol. 933, No. 1, p. 012056). IOP Publishing. https://doi.org/10.1088/1757-899X/933/1/012056.

Syukri, M., Saad, R., & Fadhli, Z. (2020b). Capability of P-and S-wave seismic refraction in delineating the Blang Bintang Sanitary Landfill (TPA) ground subsurface. *Songklanakarin J. Sci. Technol*, *42*, 780-787.

Syukri, M., Nordiana, M, M., Ismail, N, A., Fadhli, Z., Saad, R (2021). Identifying Shallow Subsurface Characteristic Via Compressional to Shear Waves Velocoty Ratio (VP/VS) From Seismic Refraction Tomography, *Jurnal Teknologi (Sciences & Engineering)*, *83*(1), 67-73. https://doi.org/10.11113/jurnalteknologi.v83.14990.

Syukri, M., Anda, S. T., Umar, M., Meilianda, E., Saad, R., Fadhli, Z., & Safitri, R. (2022). Identification of tsunami deposit at Meulaboh, Aceh (Indonesia) using ground penetrating radar (GPR). *GEOMATE Journal*, *23*(96), 171-178. https://doi.org/10.21660/2022.96.j2261.

Supriyatno. (2022). Analisa Daya Dukung Tanah Berdasar Data: Sondir, N-SPT dan Laboratorium (Studi Kasus di BTN Hamzy Makassar) Supriyanto , *Jurnal Teknik Sipil Universitas Borobudur*, pp. 105–114.

Tao, Z., Shu, Y., Yang, X., Peng, Y., Chen, Q., Zhang, Q., (2020). Physical model test study on shear strength characteristics of slope sliding surface in Nanfen open-pit mine, *International Journal of Mining Science and Technology*, Vol.30, No.3, pp. 421–429. https://doi.org/10.1016/j.ijmst.2020.05.006.

Tehrani, F, S., Calvello, M., Liu, Z., Zhang, L., Lacasse, S., (2022). *Machine learning and landslide studies: recent advances and applications*, *Natural Hazards*. Springer Netherlands. Available at: https://doi.org/10.1007/s11069-022-05423-7.

Tezcan, S.S., Keceli, A. and Ozdemir, Z. (2006) Allowable bearing capacity of shallow foundations based on shear wave velocity, *Geotechnical and Geological Engineering*, Vol.24, No.1, pp. 203–218. https://doi.org/10.1007/s10706-004-1748-4.

Tezcan, S.S. and Ozdemir, Z. (2012) Allowable Bearing Pressure in Soils and Rocks through Seismic Wave Velocities, *Earth Science Research*, Vol.1, No.1, pp. 98–108. Available at: https://doi.org/10.5539/esr.v1n1p98.

Tezcan, S.S., Ozdemir, Z. and Keceli, A. (2009). Seismic technique to determine the allowable bearing pressure for shallow foundations in soils and rocks, *Acta Geophysica*, Vol.57, No.2, pp. 400–412. https://doi.org/10.2478/s11600-008-0077-z.

Tunusluoglu, M.C. (2023). Determination of Empirical Correlations between Shear Wave Velocity and Penetration Resistance in the Canakkale Residential Area (Turkey), *Applied Sciences (Switzerland)*, Vol.13, No.17. https://doi.org/10.3390/app13179913.

Turner, A.K. (2018). Social and environmental impacts of landslides, *Innovative Infrastructure Solutions*, Vol.3, No.1, pp. 25–27. https://doi.org/10.1007/s41062-018-0175-y.

Yerro, A., Alonso, E.E. and Pinyol, N.M., (2016). Run-out of landslides in brittle soils, *Computers and Geotechnics*, Vol.80, pp. 427–439. https://doi.org/10.1016/j.compgeo.2016.03.001.

Yu, G., Sun, W. and Wang, D., (2024). Study on the shear resistance characteristics of clay-stone mixtures under freeze-thaw cycles based on nuclear magnetic resonance, *Advances in Engineering Technology Research*, Vol.10, No.1, p. 322. https://doi.org/10.56028/aetr.10.1.322.2024.

Zaini, N., Yanis, M., Marwan., Isa, M., Meer, F, D., (2021). Assessing of land surface temperature at the Seulawah Agam volcano area using the landsat series imagery, *Journal of Physics: Conference Series*, Vol.1825, No.1. https://doi.org/10.1088/1742-6596/1825/1/012021.

Zhang, N., Arroyo, M., Cintia, M, O., Gens, A., (2021). Energy balance analyses during Standard Penetration Tests in a virtual calibration chamber, *Computers and Geotechnics*, 133(February), p. 104040. https://doi.org/10.1016/j.compgeo.2021.104040.

Artikel Masuk : 14-06-2025 Artikel Diulas : 19-06-2025 Artikel Diterima : 11-08-2025

Monteiro Santos, F.A., Mateus, A., Figueiras, J. dan Gonçalves, M.A., (2006). Mapping groundwater contamination around a landfill facility using the VLF-EM method — A case study, *Journal of Applied Geophysics*, Vol.60, No.2, pp. 115–125. http://doi.org/10.1016/j.jappgeo.2006.01.002.

Artikel Masuk : 14-06-2025 Artikel Diulas : 19-06-2025 Artikel Diterima : 11-08-2025